Multiphoton ionization of magnesium via an autoionizing state

N. J. van Druten
FOM–Institute for Atomic and Molecular Physics, Kruislaan 407, 1098 SJ Amsterdam, The Netherlands

R. Trainham
FOM–Institute for Atomic and Molecular Physics, Kruislaan 407, 1098 SJ Amsterdam, The Netherlands and LI2A, Bâtiment 10-05, Centre d'Etudes Nucléaires de Grenoble, 38054 Grenoble, Cedex 9, France

H. G. Muller
FOM–Institute for Atomic and Molecular Physics, Kruislaan 407, 1098 SJ Amsterdam, The Netherlands
(Received 25 February 1994)

Multiphoton single and double ionization of magnesium was studied by measuring electron energy spectra and ion mass spectra using 1-ps laser pulses in the 580–595-nm wavelength and 10^{12}–10^{13}-W/cm^2 intensity range. In single ionization the $(3p)^2\,{}^1S$ doubly excited autoionizing state, resonant at the four-photon level, is found to play an important role. Single ionization leaving the Mg^+ ion in the $3p$ excited state is strongly enhanced when resonant with the $(3p)^2\,{}^1S$ state. The amount of above-threshold ionization observed also varies strongly in the wavelength range under study. At an intensity of 2×10^{13} W/cm^2, sequential double ionization is found to occur dominantly via the excited ionic state $Mg^+(3p)$. The first ionization step populates this state less than the ion ground state, $Mg^+(3s)$, but this is compensated by the lower order of the second ionization step.

PACS number(s): 32.80.Rm, 32.80.Dz, 42.50.Hz

I. INTRODUCTION

The advent of intense light sources in the past decades has made it possible to study photoionization of atoms in situations where a large number of photons is required to remove an electron from the atom, i.e., multiphoton ionization [1]. One of the new effects which has received considerable attention over the years is multiphoton *double* ionization [2–12], i.e., the removal of two electrons from the atom in cases were multiphoton absorption is needed for each ionization stage. The main goal of this research has traditionally been to find clear experimental evidence for so-called *direct* double ionization, the effect that two electrons are removed from the atom simultaneously via some cooperative process. This is in contrast to *sequential* double ionization, where the atom is doubly ionized in a sequence of separate ionization events, with a singly charged ion plus a free electron as an intermediate state.

This interest originates from some of the earliest experiments on multiphoton double ionization of atoms [13]. It was found that the yield of doubly charged ions was surprisingly large compared to the singly charged ion yield [14]. Furthermore, in the study of the intensity dependence of double ionization of Xe, it was found that the rate at which doubly charged ions were created saturated at the intensity where the presence of ground-state atoms was depleted by single ionization [5]. This was interpreted as evidence for direct double ionization, since the process apparently only occurred when neutral atoms were still present in the laser focus. Other explanations (see, e.g., Refs. [1,3]) are possible for these early results, as will be discussed below.

The various processes leading to multiphoton double ionization are depicted schematically in Fig. 1. The simplest form of sequential double ionization is labeled (a). It consists of single ionization of an atom A to the ground

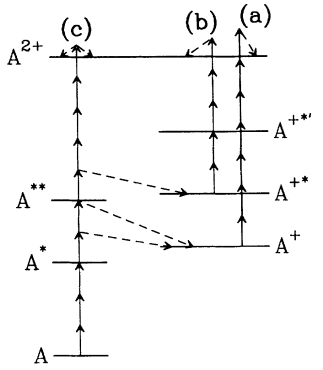

FIG. 1. Schematical energy level diagram, indicating various multiphoton processes leading to double ionization of an atom A. The upward arrows indicate photoabsorption, the downward dashed arrows indicate the emission of an electron (i.e., ionization). Path (a) is sequential double ionization via the ionic ground state A^+, (b) sequential double ionization via an excited ionic state A^{+*}, (c) direct double ionization.

state of the ion A^+, followed by a second ionization step, creating the doubly charged ion A^{2+}. This is not, however, the only possibility. In general single ionization can also leave the ion in an excited state A^{+*} from which subsequent (second) ionization is possible [the process labeled (b) in Fig. 1]. Furthermore, as multiphoton ionization usually requires high intensities, above-threshold ionization (ATI, the absorption of more photons than the minimum required for ionization) is likely, so that it becomes energetically possible to populate ionic states that are more than one photon energy above the ground state of the ion. The branching ratio to the various allowed ionic states will depend on the electron-electron interaction, i.e., on the character of the (multielectron) wave function after the absorption of a certain number of photons. In this paper, we will present results that show that in the case of magnesium and 1-ps laser pulses it is possible to populate an excited ionic state that is more than two photon energies above the ionic ground state. In addition, we find that sequential double ionization is dominated by the contribution of this excited ionic state, although single ionization dominantly populates the ground state of the ion.

Direct double ionization [path (c) in Fig. 1] can be regarded as a generalization of single ionization to an excited ionic state, the excited ionic state being a continuum state (consisting of a doubly charged ion and a second, free electron). This point of view also explains the difference in the electron spectrum that is expected between direct and sequential double ionization. In sequential double ionization the initial and final state of the core are both discrete states, in both the first and the second ionization stage. Energy conservation thus requires that, after the absorption of a number of photons, the photoelectrons have a discrete energy [15]. In direct double-ionization, on the other hand, the final state of the core in the "first ionization" process includes a second free electron, and thus consists of a continuum of energy levels. Therefore the individual electrons can have a continuous energy distribution, and only their total energy is fixed by energy conservation. As is evident from Fig. 1, direct double ionization requires the absorption of a large number of excess photons, over the minimum number needed for single ionization. In an experimentally feasible laser pulse, the single-ionization process will usually have depleted the neutral atoms in the laser focus before the light intensity has increased sufficiently to drive the direct double-ionization process [16]. As laser technology improved, shorter and shorter pulse durations were used to increase the intensity that could be reached before single ionization has depleted the neutral atoms. Nevertheless the search for more experimental evidence of direct double ionization has lead to the conclusion that sequential ionization is by far the dominant process in a large majority of cases. This also applies to the results presented here.

It is now generally accepted [1,3] that the early results on Xe and other early experiments on rare gases that seemed to indicate nonsequential double ionization (e.g., Ref. [7]) can be explained by sequential double ionization, with some (unidentified) autoionizing state as an intermediate resonance, and possibly with some excited ionic state as intermediate state. The tentative explanation is that at low intensities double ionization predominantly occurs via such an excited ionic state. The yield of doubly charged ions saturates when the neutral atoms are depleted. This yield will only increase rapidly again once ionization of the ground-state ion (also formed by the single-ionization process) becomes appreciable. Recently, additional evidence for nonsequential double ionization was found in the ion yields from irradiation of helium by 120-fs, 620-nm laser pulses [2]. The intensities are so high in this case (10^{15} W/cm^2), however, that a description in terms of tunneling ionization is more appropriate than one in terms of multiphoton absorption. Two different, simple (nonsequential) models have been proposed to explain these results [2,17].

Rare-gas atoms are particularly suited for studying the effects of very high intensities, as their large ionization potentials prevent ionization at low intensities. The alkaline-earth elements offer different advantages. They can be regarded as nearly ideal two-electron systems, and the relatively low ionization potential of both the first and the second ionization steps allow the study of multiphoton ionization at relatively low intensities. This puts less stringent demands on the laser system, and facilitates the interpretation of the results. Multiphoton single and double ionization of the alkaline-earths barium, strontium, calcium, and magnesium has been extensively studied, using ion detection, [6,8,10,11,18–22], electron spectroscopy [9,23–28] or fluorescence spectroscopy [12,29]. The general conclusion of these experiments, apart from the absence of direct double ionization [30], was that excited ionic states played an important role as intermediate states in multiphoton double ionization. Furthermore, unlike in the experiments on rare-gas atoms, most of these states could be unambiguously identified by the wavelength dependence of the ion yield, by the photoelectron spectrum or by the wavelength of the emitted fluorescence. In the case of strontium and calcium [26,29], and in the present experiment on magnesium, autoionizing states could be identified as intermediate resonances. In the case of barium, it was found that resonances in the yield of Ba^{2+} could be attributed to transitions between ionic states following single ionization [10] (the possibility of such processes is indicated by the levels A^{**} and $A^{+*'}$ in Fig. 1, respectively).

In most cases the intermediate ionic states that were populated in single ionization were found to be only a few (up to three) photons above the ionic ground state. There is one exception. Hou *et al.* [31] measured the photoelectron spectrum of multiphoton ionization of magnesium by 592-nm 30-ps laser pulses. They observed a peak at 1.2 eV and attributed it to single ionization to a highly excited ion state, at least five photons above the ion ground state. The excited ion state [$Mg^+(4p)$ or $(5p)$] is only two or three photon energies below the double-ionization limit, indicating that in this case direct double ionization would require the absorption of only a few more photons. Motivated by this result we searched for evidence of direct double ionization using the same atom and wavelength, but with a much shorter duration

(100 fs) of the laser pulse (see Ref. [32]). This was the first attempt to use an electron-coincidence technique in the search for direct double ionization. The resulting data were hard to interpret because of the large ac Stark shifts, which were due to the very short pulses used and the associated rather high intensities (10^{13}–10^{14} W/cm^2). No evidence for direct double ionization was found, and the 1.2-eV peak observed by Hou *et al.* could not be reproduced.

In the present paper, we report measurements on multiphoton single and double ionization of magnesium using 1-ps laser pulses of 580–595-nm wavelength. We have studied the wavelength dependence and intensity dependence of both the ion yield and the electron spectrum. The motivation of this research has been to investigate the anomalous behavior observed by Hou *et al.*. We feel, however, that magnesium is worth further study in itself. Its relatively simple structure of doubly excited states [almost no singlet-triplet mixing [33], the absence of an $(n-1)d$ state close to the lowest ns ionization threshold] makes an accurate theoretical description feasible. The spectroscopic position of some of the doubly excited states of magnesium has experimentally been determined in recent years [19,34,35]. Furthermore, since the ionization potential of the atom is relatively high, reasonably high intensities can be reached before the ground-state atom is depleted.

II. EXPERIMENTAL SETUP

The experiments have been performed by crossing a laser beam (focused by $f/30$ or $f/60$ optics) with a beam of magnesium atoms in a magnetic-bottle spectrometer [36]. Figure 2 gives an overview of the interaction region. A resistively heated oven (typical temperature: 700 K) with 2-mm diameter nozzle and skimmer provides an atomic beam of magnesium. The interaction region is surrounded by a copper cup, which has holes for the magnetic pole pieces, the laser light path, and for the atomic-beam skimmer. This cup is cooled by liquid nitrogen and serves to capture the atomic beam. Background pressure in the interaction region was 2×10^{-6} Pa, the magnesium pressure in the focus was estimated to be 10^{-5} Pa.

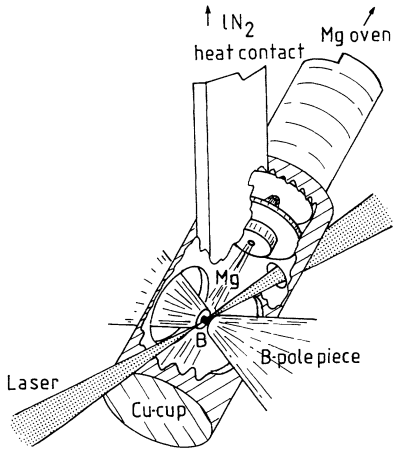

FIG. 2. The interaction region in the magnetic-bottle spectrometer. The laser beam crosses the magnesium atomic beam, and the resulting ions or electrons are detected. For electrons, the magnetic field serves to obtain a collection solid angle of 2π sr. The copper cup surrounding the interaction region is liquid nitrogen cooled, and captures the atomic beam.

For electron detection, the standard magnetic-bottle arrangement was used [36]: a constant 1-T magnetic field at the interaction region diverges into a 10-mT field in the 0.5-m flight tube, behind one of the magnetic pole pieces. The electrons emitted at the laser focus with a small velocity component in the direction of the flight tube are parallelized by the magnetic field and detected at the end of the flight tube by a multichannel plate (MCP). Thus the electrons emitted over a solid angle of 2π sr are collected. The potential at which the free electrons are created is defined by two conducting plates, mounted on the magnetic pole pieces. The time of flight of the electrons is used to calculate their kinetic energy. A typical energy resolution is 25 meV at 1 eV. To obtain similar resolution for higher-energy electrons, a retarding voltage could be applied on the flight tube. For high-resolution electron spectra, several data runs taken at different retarding voltages were added. The electron-energy scale was calibrated using the small cesium contamination that was present in the atomic beam (see Appendix B).

For ion detection, an extraction voltage was applied between the plates. The ions were further accelerated in the flight tube and detected by the MCP. The time of flight serves to analyze the mass to charge ratio of the ions. The mass spectrum was calibrated using multiphoton ionization of Xe by the frequency-doubled output of the Nd:YAG laser. Typical mass resolution at 24 amu (the mass of the most abundant magnesium isotope) was 0.5 amu for the nanosecond measurements and 1 amu for the picosecond measurements.

A 1-ps and a 5-ns laser system were used. A detailed description of the picosecond laser system can be found elsewhere [37]. In short, a colliding-pulse mode-locked laser, generating 100-fs pulses at 620-nm wavelength and 100-MHz repetition rate, was amplified at 10 Hz in a sequence of four Bethune-type dye cells pumped by the frequency-doubled output ($\lambda = 532$ nm) of a seeded Quanta-Ray GCR-4 Nd:YAG (yttrium aluminum garnet) laser. The resulting light was focused onto a water cell creating a continuum of light throughout the visible part of the spectrum. Using a pulse shaper [37] a 0.5-nm bandwidth part of this light was selected. The central wavelength of this part could be varied in the 580–595-nm range by rotating the grating in the pulse shaper. The resulting light was then amplified in a second chain of three Bethune-type dye cells. Finally, the light passed through a prism-compressor compensating for the dispersion in the amplification chain. The wavelength was calibrated with an accuracy of 0.1 nm using a 0.5-m single grating spectrometer (SPEX 1870). The pulse duration was measured to be 1.2 ps full width at

half maximum independent of wavelength and intensity. The maximum pulse energy was 200 μJ, including $\lesssim 1\%$ amplified spontaneous emission [37].

The nanosecond laser system consists of a Quantel TDL-50 dye laser, pumped by approximately 100 mJ of the frequency-doubled output of a Quanta-Ray GCR-6 Nd:YAG laser. The characteristics of the dye laser were output at dye maximum 10 mJ ($\lesssim$ 1% fluorescence), pulse duration $\approx$ 5 ns, bandwidth $\approx$ 0.003 nm. The wavelength was calibrated with an accuracy of 0.01 nm using a LambdaScope spectrometer. The light was sent through a Fresnel rhomb and a Glan-laser polarizer to keep the average output power constant when scanning the wavelength.

The energy of the laser pulses was monitored by a photodiode. The MCP and photodiode signal were collected by a digital oscilloscope, and transferred to a personal computer. The data were binned into several laser-intensity windows on the basis of the single-shot photodiode signal. The data have not been corrected for a possible time of flight or energy dependence of the collection efficiency, but such corrections are expected to be small. Count rates were kept below 20 per shot, to avoid space-charge problems.

III. RESULTS AND DISCUSSION

In the following subsections the results will be presented and discussed. We first show, in Sec. III A, that the multiphoton ionization rate of magnesium is strongly enhanced by a four-photon resonance with the $(3p)^2\ ^1S$ doubly excited, autoionizing state, when using 1-ps laser pulses. A similar measurement using 5-ns laser pulses is also presented, and confirms our interpretation of the 1-ps data. Next, in Sec. III B, the branching ratios for the various multiphoton processes leading to single ionization are determined from the electron energy spectra. It is shown that single ionization leaving the Mg^+ ion in the $3p$ excited state is strongly enhanced when resonant with the above-mentioned autoionizing state. In addition, the amount of above-threshold ionization to the ionic ground state, $Mg^+(3s)$, is found to vary strongly in the 580–595-nm wavelength range under study.

Double multiphoton ionization is discussed in Sec. III C. We show that it dominantly occurs via the $Mg^+(3p)$ excited state at an intensity of 2×10^{13} W/cm^2. Finally, in Sec. III D, our results are compared with those of Hou *et al.* [31], measured under similar conditions. A summary of the relevant energy levels of magnesium, taken from [19] and [33], is given in Fig. 3. Only singlet states have been indicated, since the ground state of magnesium is a singlet state, and, as mentioned in the Introduction, singlet-triplet mixing is known to be very small in magnesium.

A. Multiphoton single-ionization yields

We measured electron spectra and ion yields using the picosecond laser, at $\approx$ 1-nm intervals in the wavelength region 580–595 nm, with a peak intensity in the laser focus of 2×10^{12} W/cm^2. The laser was focused using $f/60$ optics in this case. Typical examples of the spectra are shown in Figs. 4(a) and 4(b). Both ion and electron spectra show a clear peak due to four-photon ionization of magnesium [38]:

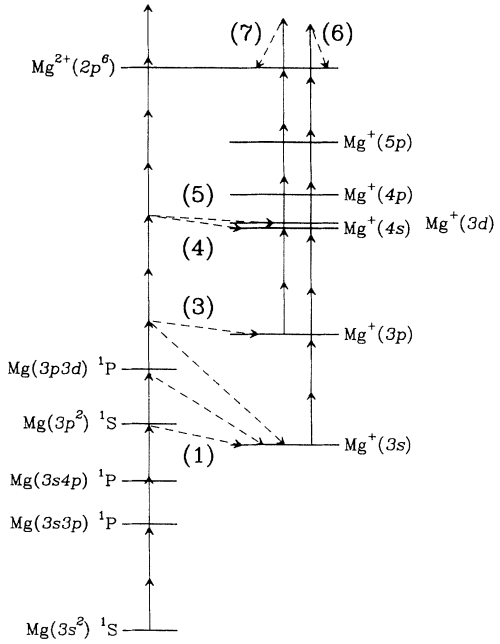

FIG. 3. Relevant energy levels (taken from [33] and [19]) and possible ionization paths of Mg and Mg^+, for a photon energy of 2.1 eV. The numbers correspond to the equations in the text.

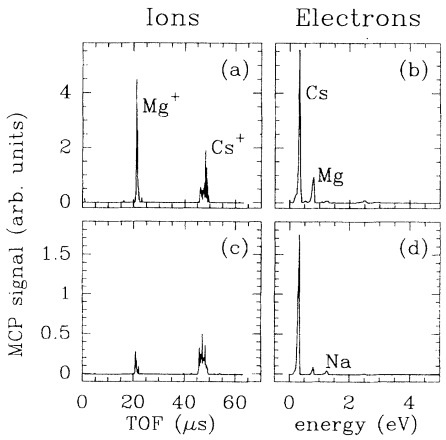

FIG. 4. Ion time-of-flight spectra [(a) and (c)] and photoelectron spectra [(b) and (d)] taken at two different intensities. The peak intensity in the laser focus was 2×10^{12} W/cm^2 for (a) and (b) and 1×10^{12} W/cm^2 for (c) and (d). The sources of the various peaks are indicated.

$$Mg(3s^2) + 4\hbar\omega \rightarrow Mg^+(3s) + e^-(0.75\ \text{eV}). \quad (1)$$

From the ion mass spectra it is clear that not only magnesium atoms are ionized in the laser focus. We attribute the other strong ion and electron peak to two-photon ionization of contaminant atomic cesium:

$$Cs(6s) + 2\hbar\omega \rightarrow Cs^+(5p)^6 + e^-(0.31\ \text{eV}). \quad (2)$$

This cesium contamination provides a good initial calibration of the electron-energy scale, as will be discussed in more detail in Appendix B. The relative amount of cesium in the atomic beam is quite small, as will become clear in later sections. It dominates the spectra here because of the low peak intensity and the lower order of the cesium ionization process.

The strength of the Mg^+ ion peak and the 0.8 eV electron peak have been plotted as a function of wavelength in Figs. 5(a) and 5(b), respectively. A clear, but broad (5 nm), resonance is observed around 591 nm. There are no known (bound) states [33] that could give rise to a one-, two-, or three-photon resonance from the magnesium ground state in this wavelength range. The known states at the four- and five-photon level (taken from Refs. [19,33,35]) have been indicated by lines in Fig. 5(d). Of those states $3p3d\ ^3D$ is very unlikely to be excited from the ground state because it is a triplet state.

Therefore the most likely candidate for the state enhancing the ionization rate is the $(3p)^2\ ^1S$ autoionizing state. The energy above the atomic ground state and the autoionization width of this state have been accurately measured to be 68 268 cm^{-1} and 278 cm^{-1}, respectively, using one- and two-photon spectroscopy [19,35]. This corresponds to a resonance position of 585.9 nm and a width of 2.5 nm in four-photon excitation. We attribute this difference between the observed position and the spectroscopically known position of this resonance to the ac Stark shift of the $(3p)^2\ ^1S$ state (Appendix A contains a discussion of the ac Stark effect). To verify that this interpretation is correct, we repeated the same measurement at different intensities. At intensities higher than that of Fig. 5(a) the magnesium ionization yield saturates, and the resonance enhancement broadens so that the yield is only weakly dependent on wavelength in the 580–595-nm range. From these observations, we estimate the saturation intensity of single ionization to be 3×10^{12} W/cm^2, consistent with the value of the four-photon ionization cross section of magnesium determined in Ref. [39].

When the intensity is decreased, the count rate drops rapidly, and the resonance position is indeed found to shift to shorter wavelengths, closer to the expected position for $(3p)^2\ ^1S$. As an example, Fig. 5(c) shows the electron yield in the 0.8 eV peak when the intensity was reduced to 9×10^{11} W/cm^2. The resonance peak is then found at 590 nm. Unfortunately measuring at even lower intensities was too difficult with this pulse duration because of the decrease in count rate.

We attribute the electron peak at 1.2 eV, visible in the electron spectrum taken at this intensity [shown in Fig 4(d)], to a tiny sodium contamination in our atomic beam. This contamination is not visible in the ion spectrum because the $^{23}Na^+$ contribution was not separable from the $^{24}Mg^+$ peak in this experiment. Multiphoton ionization of Na at these wavelengths, and similar intensity and pulse duration has recently been measured [40]. For our purposes it is sufficient to know that ioniza-

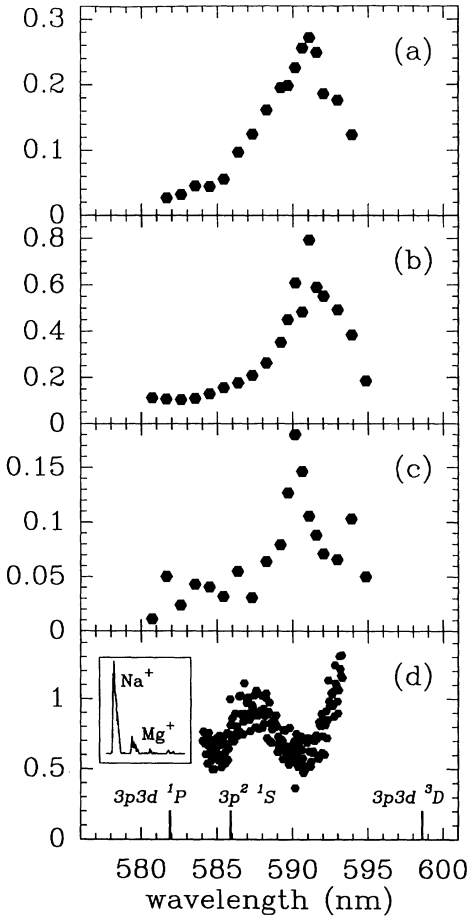

FIG. 5. The wavelength dependence of the magnesium ionization yield, for different intensities I and pulse durations τ. (a) $I = 2 \times 10^{12}$ W/cm^2, $\tau = 1$ ps, Mg^+ ion yield; (b) $I = 2 \times 10^{12}$ W/cm^2, $\tau = 1$ ps, 0.8-eV electron yield (due to four-photon ionization of magnesium); (c) $I = 1 \times 10^{12}$ W/cm^2, $\tau = 1$ ps, 0.8-eV electron yield; (d) $I = 2 \times 10^{11}$ W/cm^2, $\tau = 5$ ns, Mg^+ ion yield. Possible multiphoton resonances from the magnesium ground state are indicated in (d). The $(3p)^2\ ^1S$ state is four-photon resonant, the other two states are five-photon resonant from the magnesium ground state at the indicated position (disregarding ac Stark shifts). For decreasing intensity, the observed ionization enhancement clearly converges to the $(3p)^2\ ^1S$ position. The inset in (d) shows part of the ion spectrum taken at a wavelength of 588 nm under the same conditions as the wavelength scan in (d). The Na^+ yield is strong (mass 23 amu), but the magnesium ion yield is still well separated. Apart from the most abundant magnesium isotope (24 amu), the other magnesium isotopes with masses 25 and 26 amu (natural abundance $\approx 10\%$) are visible.

tion of sodium is completely saturated at this intensity and that the resulting electrons indeed have an energy of approximately 1.2 eV. Note that the Na contamination makes an accurate determination of the Mg ionization yield from the ion spectra [as in Fig. 5(a)] impossible at this intensity. The wing of the Na^+ peak extends to longer flight times, also contaminating the signal due to the heavier isotopes of magnesium ($^{25}Mg^+$ and $^{26}Mg^+$, natural abundance $\approx 10\%$ each).

To verify that for lower intensities the observed resonance position moves even closer to the expected position, we performed a similar experiment using the nanosecond dye laser. In this experiment we obtained an improved ion-mass resolution. The relevant part of the measured ion spectrum is shown in the inset of Fig. 5(d). This spectrum clearly shows the sodium contamination, which at this pulse duration and intensity totally dominates the ion spectrum. As a result of the good mass resolution in the case of the nanosecond laser, we were able to measure the wavelength dependence of the ionization yield of magnesium from the ion spectra again. The result is shown in Fig. 5(d). The peak intensity in the laser focus was 2×10^{11} W/cm^2 in this case. The resonance is now found at a position of 587.5 nm, with a width of 2.5 nm, indeed closer to the expected values. Note that the resonance enhancement we observe due to the $(3p)^2\ ^1S$ state is only a factor of two in the case of nanosecond pulses, whereas it is more than a factor of five for picosecond pulses. The rise in yield beyond 592 nm in Fig. 5(c) has been observed before [39] and is due to the wing of the three-photon resonance to the $3s4p$ state at 608 nm. The autoionizing resonance we observe was not found in [39], probably because of the very small resonance enhancement for the longer pulse duration (30 ns) used in that experiment.

The observation of the $(3p)^2\ ^1S$ state around 591 nm at an intensity of 2×10^{12} W/cm^2 shows that this state is ac Stark shifted to lower energies by 0.1 eV. The main contribution to the ac Stark shift of this state is expected [41] to be due to coupling with the $3p3d\ ^1P$ state at 85 925 cm^{-1} [33]. The (one-photon) coupling between these two states by the light field is near resonant, with a negative detuning of 600 cm^{-1}. This "pushes" the $(3p)^2\ ^1S$ state down. If this coupling also dominates the ac Stark shift of the $3p3d\ ^1P$ state, the latter state will show a positive ac Stark shift (i.e., to shorter wavelengths), and possibly moves out of our wavelength range. This could explain why we do not observe the $3p3d\ ^1P$ state as a resonance in the ion-yield measurements. We speculate that the resonance observed in Ref. [32] at 598 nm, using 100-fs pulses (and higher intensities), is also due to the $(3p)^2\ ^1S$ state, shifted even further to lower energies.

B. Branching ratios in single ionization

In order to obtain more information on single ionization of magnesium, we used $f/30$ optics to focus the light more tightly to reach intensities of $\approx 10^{13}$ W/cm^2, where the single ionization of magnesium is saturated. Typical results for the electron spectra are shown in Fig. 6. The

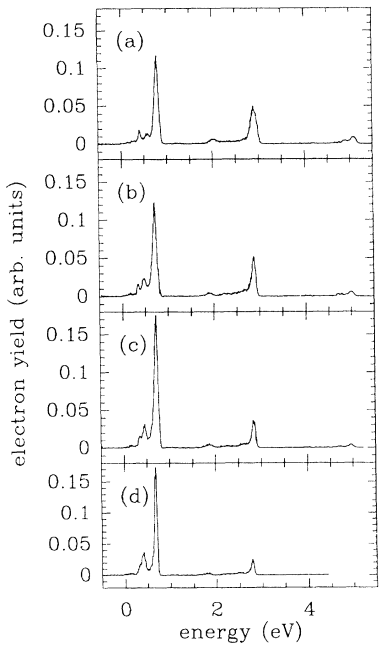

FIG. 6. Photoelectron spectra of Mg, irradiated by a 1-ps pulse of laser light with wavelength λ. (a) $\lambda = 581.7$ nm. (b) $\lambda = 587.3$ nm. (c) $\lambda = 590.1$ nm. (d) $\lambda = 593.0$ nm. The peak intensity in the focus was 1×10^{13} W/cm^2.

spectra consist of a number of peaks shifting slightly in energy when the wavelength is varied. An example of the intensity dependence of the electron spectra for $\lambda = 590.1$ nm is shown in Fig. 7. The intensity dependence at other wavelengths was found to be similar. A typical ion time-of-flight spectrum at this intensity is shown in Fig. 8.

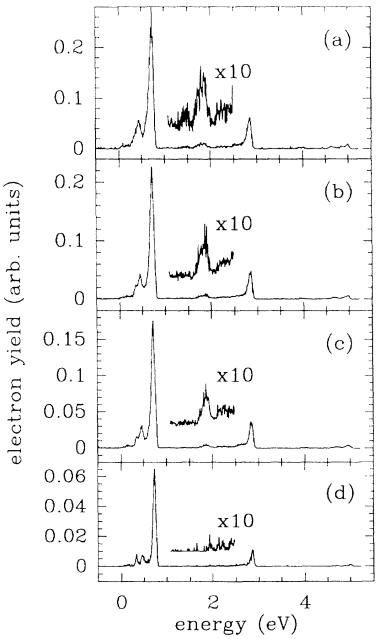

FIG. 7. Intensity dependence of the photo electron spectra of Mg, irradiated by a 1-ps laser pulse with a wavelength of 590.1 nm. (a) $I = 34 \times 10^{12}$ W/cm^2. (b) $I = 18 \times 10^{12}$ W/cm^2. (c) $I = 10 \times 10^{12}$ W/cm^2. (d) $I = 3 \times 10^{12}$ W/cm^2. The spectrum between 1 and 2.5 eV is also shown with an enlarged vertical scale (and a vertical offset).

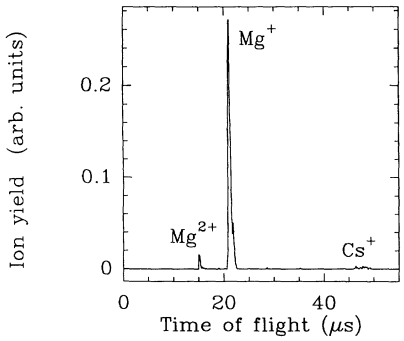

FIG. 8. Typical ion mass spectrum taken at an intensity of $I = 1 \times 10^{13}$ W/cm^2. The laser wavelength was 588 nm in this case, the pulse duration was 1 ps.

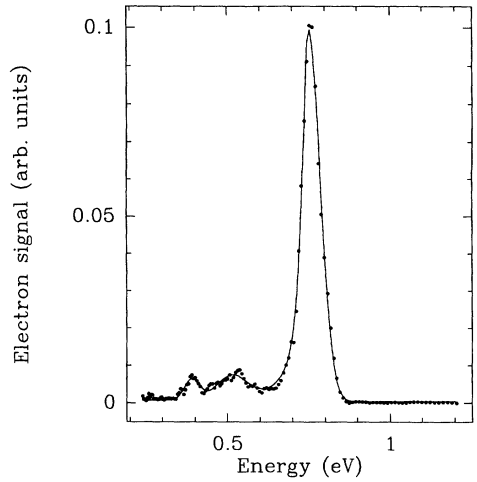

FIG. 9. Example of a part of the electron spectrum (measured at $\lambda = 586.4$ nm, and $I = 1 \times 10^{13}$ W/cm^2) and the fit to it using the peak shapes described in the text. The points are the measured data, the solid line is the fit.

Mg^+ is by far the dominant ion produced, but some Mg^{2+} is also clearly visible [42]. The relative importance of the cesium contamination is reduced significantly. The ion time-of-flight spectrum was found to depend only weakly on wavelength. When the intensity was varied, the Mg^+-ion yield was indeed found to be saturated. The relative importance of the Mg^{2+} peak increased with intensity.

To accurately determine the positions, strengths, and widths of the observed peaks in the electron spectra, we fitted functions to the spectra, as follows: Gaussians were fitted to the well-separated peaks around 3 eV and 5 eV. For the three closely spaced peaks between 0 and 1 eV two Gaussian functions (for the two small low-energy peaks) and a function consisting of a Lorentzian low-energy side and a Gaussian high-energy side (for the largest peak) were fitted simultaneously. The asymmetry in the function fitted to the largest peak was found to be necessary to correctly fit the weaker ones. Although there is no *a priori* justification for these peak shapes, this choice was found to represent the electron spectra sufficiently well to extract the desired data. An example of such a fit for the 0–1 eV-region is shown in Fig. 9. The peak positions found from the fits to the electron spectra, for an intensity of 1×10^{13} W/cm^2, are plotted in Fig. 10 as filled hexagons. In addition, straight lines were fitted to these peak positions as a function of the photon energy. The results are shown as drawn lines in Fig. 10. The slope and position of these lines is given separately in Table I. To connect these results with the low-intensity data presented in Sec. III A, we also fitted Gaussians to the three peaks visible in Fig. 4(d). The resulting positions, and the lines fitted to the wavelength dependence, are also shown in Fig. 10, using open hexagons.

Our interpretation of the various peaks in the electron spectra is based on their position, wavelength dependence, and intensity dependence. The dashed lines in Fig. 10 indicate the expected electron energies for various multiphoton ionization processes [38]. In Fig. 10 the low-intensity peaks (the open symbols) are found on or near the expected lines for cesium, magnesium, and sodium respectively, confirming our interpretation of the three electron peaks visible at low intensities [Fig. 4(d)]. The main discrepancy, a small upward shift of the observed sodium peak, is consistent with the recent measurement

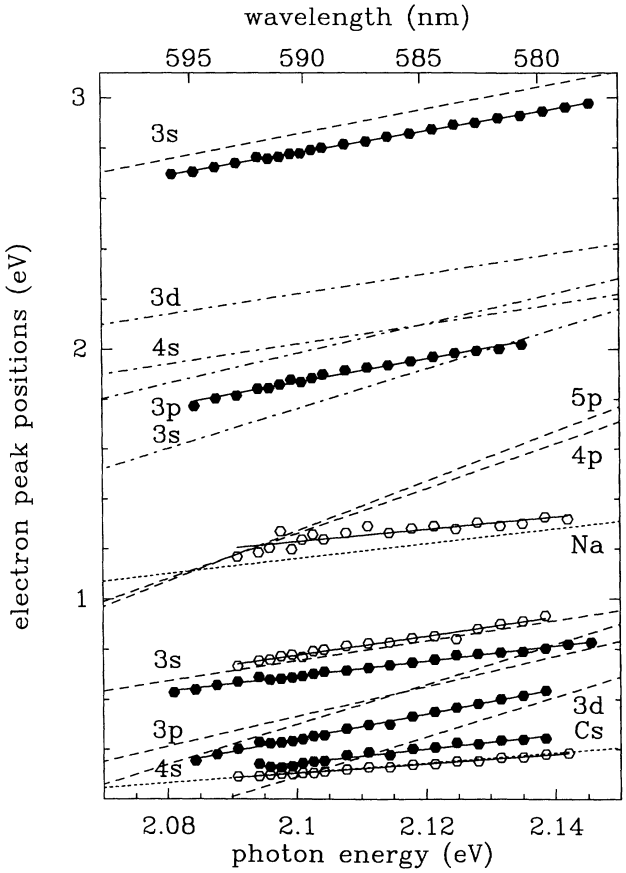

FIG. 10. Electron peak positions as a function of photon energy. The points are observed peak positions, the solid lines are linear fits to the observed wavelength dependence. The broken lines indicate expected positions (disregarding possible ac Stark shifts) for the processes discussed in the text. Single ionization of magnesium is indicated by dashed lines, labeled with the ionic state to which ionization takes place. Second ionization from these excited ionic states is indicated by dashed-dotted lines. The dotted lines indicate the expected electron energies for the contaminations found.

TABLE I. Overview of the electron peaks found in the experimental electron energy spectra. Each peak is represented by the line that was fitted to its photon-energy-dependent position (see Fig. 10). Slope N_{expt} and position (at $\hbar\omega = 2.1$ eV) of the lines are given, as well as the intensity at which these positions were measured. The numbers in parentheses indicate the estimated uncertainty in the last digit. The column labeled "Eq." refers to the numbered equations in the text ("Na" indicates sodium), to which we have assigned the peaks, with the absorption of N photons.

I (TW/cm^2)	N_{expt}	E (eV)	Eq.	N
0.8	3.8(5)	0.78(2)	1	4
10	3.0(5)	0.71(2)	1	4
10	4.4(5)	2.78(4)	1	5
10	5.0(5)	0.44(2)	3	6
20	4.7(5)	1.87(4)	7	6
0.2	1.9(2)	0.31(2)	2	2
10	2.8(5)	0.35(2)	2	2
0.8	3(1)	1.25(5)	Na	3

of multiphoton ionization of sodium in this wavelength and intensity range by Papaioannou and Gallagher [40].

In the electron spectra taken at higher intensities, the sodium peak is no longer visible, and the cesium and magnesium peaks are found shifted from their low-intensity position. This shift is due to the ac Stark shift of the initial and final states involved. We have calculated these shifts (see Appendix A), the result of this calculation is given in Table II. The observed shift of the cesium and magnesium peaks is in reasonable agreement with the calculation, taking into account that the ionization has already saturated below the maximum intensity in the focus. The decrease in shift towards longer wavelengths of the main magnesium peak nicely corresponds to the decrease in saturation intensity caused by the resonance observed in Sec. III A. The peaks at 3 and 5 eV are due to above-threshold ionization of the process of Eq. (1), with five and six photons, respectively, instead of four. These peaks are found shifted down by a similar amount. This ATI series continues to higher energies (not shown), but the strength of the peaks rapidly decreases. The electron yield above 5.3 eV was found to be less than 2% of the total electron yield in the electron spectra studied here.

An additional peak around 0.5 eV is found in the high-intensity electron spectra. As shown in Fig. 7 it becomes relatively more important at higher intensities, eventually masking the cesium peak. No contamination ions were observed in the ion time of flight that could give rise to this peak (see Fig. 8), and we conclude that it must be due to single ionization of magnesium to an excited state of the ion. As mentioned in the introduction such behavior has been observed before in high-intensity multiphoton ionization of the alkaline-earth elements. The identification of the final ionic state to which this peak corresponds is obviously hampered by the occurence of ac Stark shifts. We presume, by the rapidly decreasing strengths of the ATI peaks in the photoelectron spectra, that only the lowest excited states are probable candidates, because they require fewer photons. To be specific, populating the first excited ionic state, $Mg^+(3p)$, is possible by the absorption of six photons:

$$Mg(3s)^2 + 6\hbar\omega \rightarrow Mg^+(3p) + e^-(0.53\ \text{eV}). \quad (3)$$

Only after absorption of an additional two photons will other ionic excited states become energetically accessible, namely, $Mg^+(4s)$ and $Mg^+(3d)$:

$$Mg(3s)^2 + 8\hbar\omega \rightarrow Mg^+(4s) + e^-(0.50\ \text{eV}), \quad (4)$$

TABLE II. Properties of the multiphoton ionzation processes discussed in the text. Eq. refers to the numbered equations in the text. IP is the ionization potential of the process (without ac Stark shifts), taken from Refs. [33] and [47], with a conversion factor of 8065.541 cm^{-1}/eV. N_{min} is the minimum number of 2.1-eV photons needed for ionization and E_0 the kinetic energy of the resulting electron, at zero intensity of the light field. $\Delta E/I$ is the expected shift coefficient of the electron energy with light intensity, due to ac Stark shifts (see Appendix A), the numbers in parentheses indicate the estimated error in the last digit. The fine structure in the initial and final states (due to spin-orbit interaction) is sufficiently small (≤ 0.01 eV) in all these cases, so that it can be neglected. In the case of sodium an ac Stark *splitting* is expected, instead of a shift [40].

Eq.	initial state	final state	IP (eV)	N_{min}	E_0 (eV)	$\Delta E/I$ [eV/(TW/cm^2)]
1	$Mg(3s)^2$	$Mg^+(3s)$	7.65	4	0.75	-0.043(4)
3	$Mg(3s)^2$	$Mg^+(3p)$	12.08	6	0.53	-0.044(4)
4	$Mg(3s)^2$	$Mg^+(4s)$	16.30	8	0.50	-0.13(2)
5	$Mg(3s)^2$	$Mg^+(3d)$	16.51	8	0.29	-0.019(4)
	$Mg(3s)^2$	$Mg^+(4p)$	17.64	9	1.26	
	$Mg(3s)^2$	$Mg^+(5p)$	19.73	10	1.27	
6	$Mg^+(3s)$	$Mg^{2+}(2p)^6$	15.04	8	1.76	-0.042(3)
7	$Mg^+(3p)$	$Mg^{2+}(2p)^6$	10.62	6	1.98	-0.041(4)
8	$Mg^+(4s)$	$Mg^{2+}(2p)^6$	6.38	4	2.02	+0.05(2)
9	$Mg^+(3d)$	$Mg^{2+}(2p)^6$	6.17	3	0.13	-0.066(4)
2	$Cs(6s)$	$Cs^+(5p)^6$	3.89	2	0.31	+0.043(4)
	$Na(3s)$	$Na^+(2p)^6$	5.14	3	1.16	

and

$$\mathrm{Mg}(3s)^2 + 8\hbar\omega \rightarrow \mathrm{Mg}^+(3d) + e^-(0.29\ \mathrm{eV}). \quad (5)$$

It requires the absorption of two more photons (i.e., ten photons total from the Mg ground state) before other Mg^+ states giving rise to electrons in the 0.5-eV energy range can be populated.

The unshifted electron energies of the processes of Eqs. (3)–(5) are also shown in Fig. 10. The lowest-order process should be the most probable and the process of Eq. (3) should give, by far, the largest contribution to the 0.5-eV peak. The calculated ac Stark shift of the electron energy for Eq. (3) is consistent with this interpretation (see Table II). In addition, the observed slope of the electron energy versus photon energy (5) is closest to the value expected for Eq. (3). Note furthermore that we find no evidence in the electron spectrum of the nine-photon ionization of magnesium leading to population of the $Mg^+(4p)$ state. The latter process would result in electrons around 1.3 eV, and these are not observed in the high-intensity spectra. This indicates that single ionization of magnesium saturates at an intensity where this nine-photon process is still very unlikely. Likewise, we expect that the eight-photon processes of Eqs. (4) and (5) are very weak at these intensities. In addition, the process of Eq. (5) cannot contribute to the 0.5-eV peak, considering the sign of the calculated ac Stark shift. The unshifted electron energy for this process is below the observed energy, and the negative ac Stark shift (see Table II) should shift it even lower. It is, however, still possible that this process occurs weakly, and that the resulting electrons are hidden under the tails of the cesium electron peak around 0.3 eV. In contrast, the ac Stark shift of the electrons resulting from the process of Eq. (4) is consistent with a possible contribution to the 0.5-eV peak. We conclude that in single ionization a significant fraction of the ions is formed in the $3p$ excited state [Eq. (3)], but that minor contributions of the processes of Eqs. (4) and (5) cannot be excluded. Fluorescence spectroscopy of the excited ionic levels (as done for calcium and strontium in [12] and references therein) would be a way to distinguish the latter contributions.

The branching ratios to the various ionic states in single ionization were determined by calculating the area under the curves that were fitted to the peaks in the electron spectrum. The areas were normalized to the total electron yield at the wavelength at which they were measured, to compensate for fluctuations in the magnesium density during the measurements. The result is shown in Fig. 11(a), for an intensity of 1×10^{13} W/cm^2. Some of the relative peak strengths vary considerably in this wavelength range. The ATI series connected with Eq. (1) increases strongly towards shorter wavelength, whereas the lowest-order (four-photon) peak of the same process decreases in the same direction. Another clear feature is the strong increase in the 0.5-eV peak [the process of Eq. (3)] towards longer wavelength. For the longest wavelengths used, this six-photon process becomes comparable in strength to the first ATI peak of Eq. (1), which is a five-photon process. Note that the latter process and the second ATI peak of Eq. (1) are both six-photon processes from the same initial state, but show a complementary wavelength dependence.

As discussed in Sec. III A, we only observed one resonance in the single ionization of magnesium this wavelength regime, the $(3p)^2\ ^1S$ state, shifted by ac Stark shift from 585.9 nm to longer wavelengths. We associate the increase in the six-photon ionization to the $Mg^+(3p)$ state with this intermediate resonance. The increase in ionization to an excited ionic state due to an intermediate resonance with a doubly excited state has been observed before for other alkaline-earth elements, most notably strontium (see, e.g., Refs. [26] and [29]). In fact the detection of the fluorescence from the excited ionic states has been used in multiphoton spectroscopy of the intermediate autoionizing states.

Several explanations are possible for the the increase in ATI at shorter wavelengths. Since we move away from the three- and four-photon resonances with the $3s4p$ and $(3p)^2\ ^1S$ states, respectively, the ionization cross section

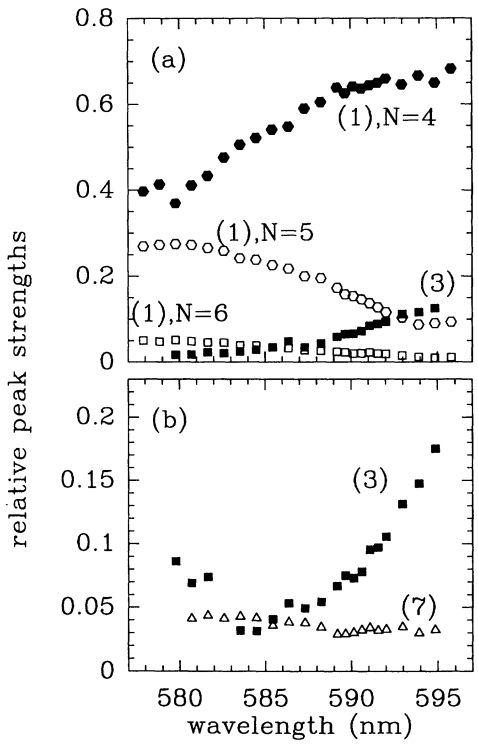

FIG. 11. Relative strengths of the electron peaks associated with single and double ionization of magnesium. The numbers indicate the equations to which we attribute the peaks. (a) $I = 1 \times 10^{13}$ W/cm^2, single ionization to the $Mg^+(3p)$ state [Eq. (3)], and single ionization to $Mg^+(3s)$ [Eq. (1)], by four-, five-, and six-photon absorption. The latter two (ATI) processes increase strongly at short wavelengths. The first process increases strongly at long wavelengths. (b) $I = 2 \times 10^{13}$ W/cm^2, sequential double ionization (triangles), and single ionization to the $Mg^+(3p)$ state. Note that the double-ionization peak is comparable in strength to the single-ionization peak.

is lower here. This implies an increased saturation intensity, and ground-state atoms can survive up to an intensity where ATI processes are more likely. On the other hand, as mentioned in Sec. III A, the $3p3d\ ^1P$ autoionizing state is nearly five-photon resonant around 582 nm. Such a resonance could enhance the five-photon ionization yield. In addition there may be other doubly excited states in five- or even six-photon resonance from the ground state. The $3p3d\ ^1F$ state, for instance, is predicted to be close to the $3p3d\ ^1P$ state [43]), but has not been observed experimentally. Possibly all these effects contribute to the observed behavior. Further experiments will be necessary to clarify this issue. In particular it would be interesting to study the strengths of the ATI peaks at shorter wavelengths. If a resonance is involved, they should decrease again. If the strengths are determined by the decrease in ionization cross section, they should increase even further.

C. Double ionization

When the intensity is increased beyond 1×10^{13} W/cm^2, a rather broad peak becomes visible around 1.9 eV. It is clearly visible in the enlarged spectra in Fig. 7. A Gaussian was fitted to this peak (at $I = 2\times10^{13}$ W/cm^2), and the wavelength dependence of the peak position and strength is shown in Fig. 10 and 11(b) respectively. We attribute this peak to sequential double ionization of magnesium. This conclusion is based on the observation that the appearance of this peak correlates well with the appearance of Mg^{2+} in the ion spectrum, and that the electron energy is close to the energies expected for sequential double ionization. The latter energies, resulting from (second) ionization of the $Mg^+(3s)$, $3p$, $4s$, and $3d$ states are denoted by dashed-dotted lines in Fig. 10. The following arguments lead to an assignment of the 1.9-eV peak to $Mg^+(3p)$.

From the electron spectrum of single ionization of magnesium, discussed in the previous section, we found that the Mg^+ ion is preferentially left in the $3s$ ground state. Subsequent ionization of this state,

$$Mg^+(3s) + 8\hbar\omega \rightarrow Mg^{2+}(2p)^6 + e^-(1.76\ \text{eV}), \qquad (6)$$

is indicated by the lowest dashed-dotted line in Fig. 10. The calculated ac Stark shift of the electrons resulting from this process is negative, whereas the electron peak found in the experiment has an energy *higher* than the zero-intensity line. We thus conclude on the basis of the calculated ac Stark shift for Eq. (6), that this process does not contribute to the observed 1.9-eV peak.

The situation is different for ionization of the $Mg^+(3p)$ state, also populated in single ionization, as we saw above. The process

$$Mg^+(3p) + 6\hbar\omega \rightarrow Mg^{2+}(2p)^6 + e^-(1.98\ \text{eV}) \qquad (7)$$

results (for low intensities) in electrons with an energy higher than observed in the experiment, but the sign and magnitude of the calculated ac Stark shift is now consistent with this difference. This process is thus a possible candidate for causing the peak around 1.9 eV. Note that ionization of $Mg^+(3p)$ [Eq. (7)] involves two photons less than that of $Mg^+(3s)$ [Eq. (6)]. The lower order of the former process could compensate for the smaller population created in the $Mg^+(3p)$ state by the first ionization step.

As mentioned in Sec. III B single ionization of magnesium to the $Mg^+(4s)$ and $Mg^+(3d)$ states cannot be excluded from our data. Ionization of these ionic states would give unshifted electron energies that are also indicated in Fig. 10. The calculated ac Stark shift of second ionization of $Mg^+(3d)$ is in the direction of the observed 1.9-eV peak. The calculated shift of $Mg^+(4s)$ is in the opposite direction. Therefore the only possible ionic states, populated in single ionization, for which ionization could lead to 1.9-eV electrons are $Mg^+(3p)$ and $Mg^+(3d)$. The latter possibility can be excluded using the peak strengths shown in Fig. 11(b). This figure shows that the 1.9-eV peak, associated with the second ionization step, can have a strength similar to that of single ionization to $Mg^+(3p)$. In Sec. III B we concluded that single ionization to the $Mg^+(3d)$ state is much weaker than to the $Mg^+(3p)$ state. These two observations imply that the observed sequential double ionization is stronger than single ionization to $Mg^+(3d)$, so that the latter cannot give the dominant contribution to double ionization. We therefore conclude that the 1.9-eV peak is due to second ionization of the $Mg^+(3p)$ state and that sequential double ionization occurs dominantly via this excited ionic state at an intensity of 2×10^{13} W/cm^2.

There are two objections that can be raised against the above conclusion: the strength of the 1.9 peak does not follow the strong variation in the population of the initial state $Mg^+(3p)$ in this wavelength range, and the slope of the position of this peak versus photon energy does not correspond very well to the order of the process of Eq. (7). Both discrepancies can be explained by the occurrence of intermediate resonances in the second ionization step as is discussed below.

The strong wavelength dependence of the population created in $Mg^+(3p)$ (by the first ionization step) can be compensated by the wavelength dependence of the second ionization step from this state. A possible cause of the latter wavelength dependence is the four-photon resonance between $Mg^+(3p)$ and $Mg^+(5f)$ at 589 nm (without ac Stark shifts). The relative ac Stark shift of these two levels can cause this resonance to be important only for wavelengths shorter than 589 nm. In addition the Mg^+ Rydberg series can be ac Stark shifted into five-photon resonance with the $Mg^+(3p)$ state. At the intensities and pulse duration used here one finds that the dynamics of the ionization process can be dominated by such weakly bound Rydberg states [44–46]. These Rydberg states shift in and out of multiphoton resonance with the initial state by the varying intensity in the laser pulse. Although the direction of the shift in the observed electron energy is in this case still given by the ac Stark shifts of the initial and final state, the intermediate Rydberg states determine at which shift the maximum electron yield occurs. The slope of electron energy versus

photon energy is then no longer a measure for the total number of photons absorbed from the initial state, but is determined by the number of photons absorbed to ionize the intermediate Rydberg state and the ac Stark shift of the latter state relative to the ionization threshold. Similar behavior in the second ionization step from $Mg^+(3p)$ can be expected, so that deviations in the observed slope are not surprising.

Our result that sequential double ionization of magnesium occurs dominantly via the $Mg^+(3p)$ state at an intensity of 2×10^{13} W/cm^2 shows that the dominant mode of (sequential) double ionization is critically dependent on the values of the various cross sections involved. Although the population created in an ionic state by single ionization decreases rapidly when the ionic state has a higher energy (due to the larger number of photons that needs to be absorbed), the second ionization step may initially compensate for this, since it requires a number of photons that is correspondingly smaller. With increasing intensity, ionization of the $Mg^+(3s)$ state would obviously dominate the Mg^{2+} production at some point, since $Mg^+(3s)$ is the most abundantly produced state in single ionization. In the intensity range we have used here, this contribution is apparently still small compared to ionization of the $Mg^+(3p)$ state. As an aside we note here that it is essential for the above considerations that the radiative lifetime of the excited ionic state be long compared to the laser pulse duration. If this is not the case, the excited ionic state will have decayed by spontaneous emission before it can be ionized. Since the radiative lifetime is a few nanoseconds for the excited Mg^+ states considered here [47] this requirement is fullfilled in the present experiment.

All the features observed here are explained without consideration of direct double ionization. The sequential ionization processes requiring eight or more photons are found to be quite weak, even at an intensity where the single ionization of magnesium is saturated. It thus seems unlikely that direct double ionization, which requires at least eleven photons, can be observable here. We conclude that double ionization is dominated by the sequential process for the intensities and pulse duration used in this experiment.

D. Comparison with Hou *et al.*

Our results partially differ from those obtained by Hou *et al.* [31] under similar experimental conditions. In their experiment Mg atoms were subjected to 30-ps laser pulses of 590.6-nm wavelength in a similar electron spectrometer. At an intensity of 8×10^{11} W/cm^2 strong peaks in the electron spectrum were found at 0.8 eV, 2.1 eV, and 3.0 eV, similar to our experiment. An additional peak at 1.2 eV was observed in [31] when the intensity was increased to 4×10^{12} W/cm^2. Hou *et al.* suggest that this additional peak is due to nine- or ten-photon excitation from the ground state of the atom to higher-lying states of Mg^+ (specifically $4p$ and $5p$). These processes have also been indicated as dashed lines in Fig. 10. Note that for the wavelength used in Ref. [31], both processes result in electrons of approximately the same energy of 1.2 eV. If this interpretation is correct, the absence of this peak in the present study is difficult to explain. Our light pulses are much shorter than those used in Ref. [31] (1 vs 30 ps), and the associated higher saturation intensities should thus favor higher-order processes. Furthermore it seems unlikely that nine- or ten-photon absorption from the atom ground state is much stronger than five-photon absorption (resulting in the ATI peak at 3 eV) at an intensity of 4×10^{12} W/cm^2, which is what is implied in Ref. [31].

We did, however, observe a peak at 1.2 eV at very low intensities, which we attribute to a tiny sodium contamination of the magnesium we used, as discussed Sec. III A. We wonder if the 1.2-eV peak observed in Ref. [31] could also be due to some contamination, maybe sodium as well, even though in Ref. [31] the 1.2-eV peak is not observed at low intensities. We feel that the interpretation of this peak given in Ref. [31] should be verified, for instance by measuring the wavelength dependence of the position of this peak. As illustrated in Fig. 10, this should distinguish unambiguously between three-photon ionization of sodium and nine- or ten-photon ionization of magnesium to the $Mg^+(4p)$ or $(5p)$ state.

The peak we observe around 0.5 eV, due to the process of Eq. (3), is not observed by Hou *et al.* However, it is suggested in Ref. [31] that this process does occur, but that the 0.5 eV peak is buried in the wing of the 0.8 eV peak in that case. This difference between the present experiment and Ref. [31] thus seems to be minor. It could be due to differences in electron-energy resolution, or in the detection efficiency of low-energy electrons.

IV. CONCLUSIONS

Multiphoton ionization of magnesium with 1-ps, $I \approx 10^{13}$ W/cm^2 light pulses of 580–595-nm wavelength shows a number of interesting aspects. The interpretation of the data is complicated significantly by the occurrence of ac Stark shifts, intrinsic to the use of high laser intensities. Careful analysis, however, has made it possible to draw definite conclusions on most of the features. The $(3p)^2\ ^1S$ autoionizing state resonantly enhances the four-photon ionization yield, and is ac Stark shifted down in energy. In single ionization the Mg^+ ion is partially left in the $3p$ excited state. The excitation of this state is strongly enhanced when being resonant with the $(3p)^2\ ^1S$ state. The above-threshold ionization probability in single ionization also shows a marked dependence on wavelength in the 580–595-nm range studied here. A study over a more extended wavelength range should give more information on this phenomenon. Although excitation of $Mg^+(4s)$ and $3d$ in single ionization cannot be excluded, the probability of these processes must be small. Contrary to Hou *et al.* [31], we do not observe the peak in the electron spectrum around 1.2 eV. We suggest that this peak be further investigated to verify the interpretation given in Ref. [31]. Sequential double ionization is found to occur dominantly via the $Mg^+(3p)$ excited state, al-

though this state is populated much less than $Mg^+(3s)$ ground state by single ionization.

ACKNOWLEDGMENTS

We thank the infrared laser group at our institute for the use of their SPEX 1870 spectrometer, J.H. Hoogenraad for software support in interfacing the Quantel TDL-50 dye laser to the computer, R. Kemper for technical support, S. Kotochigova for pointing out the relevance of the $3p3d\,^1P$ state, and P. Agostini and T.F. Gallagher for stimulating discussions. This work is part of the research program of the "Stichting voor Fundamenteel Onderzoek der Materie (FOM)" and was made possible by financial support of the "Nederlandse Organisatie voor Wetenschappelijk Onderzoek (NWO)" and the European Community through Grant No. SCI-0103C.

APPENDIX A: CALCULATION OF AC STARK SHIFTS

The energy shift ΔE of an atomic level due to the presence of a strong light field, the ac Stark shift or light shift, is in general proportional to the light intensity I,

$$\Delta E = \alpha I. \tag{A1}$$

It is convenient to discuss the ac Stark shifts of strongly bound states and of continuum states separately [48]. For a strongly bound state $|i\rangle$ with energy E_i the ac Stark shift coefficient α_i is given by second-order perturbation theory (see, e.g., Ref. [49]), in the absence of one-photon resonances. In atomic units

$$\alpha_i = \frac{1}{4}\sum_k |\langle i|D|k\rangle|^2 \left(\frac{1}{E_i - E_k + \omega} + \frac{1}{E_i - E_k - \omega}\right), \tag{A2}$$

where k sums over all other atomic states $|k\rangle$ with energy E_k (including the continuum), ω is the frequency of the light field, and D is the dipole operator. The squared matrix elements in Eq. (A2) can be calculated from the line oscillator strengths f_{ik}, which are known for the lowest bound levels [47,50]. For linear polarization [51]

$$|\langle i|D|k\rangle|^2 = \frac{3f_{ik}}{2(E_k - E_i)}(J_k 1 M_k 0 | J_k 1 J_i M_i)^2, \tag{A3}$$

where J_a and M_a denote the total angular momentum of state $|a\rangle$ and its projection on the laser polarization direction, respectively, and $(\,|\,)$ denotes a Clebsch-Gordan coefficient [52].

Since for any particular low-lying state $|i\rangle$ usually only a few levels $|k\rangle$ have appreciable oscillator strengths, the ac Stark shift of the low-lying levels can easily be estimated by taking into account only the most important levels $|k\rangle$.

For continuum states with nonrelativistic electron energies and also for weakly bound Rydberg states (which can be considered as nearly free) it is easily shown that the ac Stark shift is equal to the ponderomotive potential U_p [48,53]

$$\alpha_c = U_p/I = \frac{1}{4\omega^2}, \tag{A4}$$

where ω is the frequency of the light field. This is simply the minimum average kinetic energy of an electron quivering in a classical light field.

A free electron created in a multiphoton ionization process at an intensity I thus has a total kinetic energy that consists of this quiver part U_p, and a drift part E_d. This total energy is fixed by energy conservation:

$$E_d + U_p = E_f - E_i + n\omega, \tag{A5}$$

where n is the number of photons absorbed, and E_i and E_f are the energies of the initial and final state of the atom and the ion, respectively (or, in the second ionization step, of the singly charged ion and the doubly charged ion, respectively). The intensity dependence of the drift energy is therefore given by $\Delta E_d(I) = \alpha_d I$, with

$$\alpha_d = -\frac{1}{4\omega^2} + \alpha_f - \alpha_i. \tag{A6}$$

The electron spectra reported in this paper where measured in the short-pulse regime, i.e., the laser pulses are so short that the electrons do not move over a significant part of the laser focus within the laser pulse. Thus the electrons do not convert their quiver energy to drift energy by "surfing" off the spatially-varying ponderomotive potential created by the focused light [53]. Instead, the quiver energy is given back to the light field. Thus the measured energy of an electron is $E_d(I)$. We have calculated the shifts α_i and α_f of the various initial and final states involved, for $\hbar\omega = 2.1$ eV ($\lambda = 590.4$ nm), and the resulting α_d is given in Table II.

The fine structure splitting in $Mg^+(3p)$ of 11 meV is found to be negligible in this calculation, as well as the M_i dependence of the level shifts. The dependence of the shift on ω can also be neglected in the wavelength range studied in the experiment. In most cases the ponderomotive potential is the dominant contribution,

$$U_p/I = 0.033\ \text{eV}/(\text{TW/cm}^2). \tag{A7}$$

APPENDIX B: ELECTRON-ENERGY CALIBRATION

Calibrating the electron-energy scale is not trivial because contact potentials are relatively unknown and can even change due to magnesium deposits on the plates in the interaction region. In this experiment, the absolute electron energy was determined using the cesium contamination of the magnesium atomic beam. As shown in Sec. III A, at low intensities the main peak in the electron spectra is due to two-photon ionization of cesium [Eq. (2)]. At an intensity of 2×10^{11} W/cm^2 the ac Stark shift of this electron peak is expected to be negli-

gibly small ($\leq$ 10 mV). This energy was assumed to be equal to the expected energy of Eq. (2), for one particular wavelength, $\lambda = 587.3$ nm. This determines the effective contact potential at the interaction region, which was found to be -1.8 eV, and to fluctuate less than 0.1 eV on a day to day basis.

The open hexagons around 0.3 eV in Fig. 10 indicate the wavelength dependence of the peaks found for this electron-energy calibration. Note that the hexagons for the cesium peak lie within 10 meV of the expected line (with a slope of two). This independently shows that this peak is due to a two-photon process, confirming our interpretation of this peak. Also note that the observation of this peak in itself shows that our spectrometer transmits low-energy electrons down to an energy of (at least) 0.3 eV.

When the intensity was increased above the saturation intensity of cesium ($\approx 5 \times 10^{11}$ W/cm^2 [54]), the maximum shift observed for the cesium peak was 50 meV at $\lambda = 587.3$ nm, consistent with the calculated ac Stark shift (see Table II). This shifted position was next used for the calibration of the spectra taken at high intensities, the closed symbols in Fig. 10 ($I \approx 10^{13}$ W/cm^2). We estimate this electron-energy calibration to be correct within 30 meV at low energies, degrading to 50 meV at higher energies (above 1 eV).

[1] H. G. Muller, P. Agostini, and G. Petite, in *Atoms in Intense Laser Fields*, edited by M. Gavrila (Academic, San Diego, 1992), pp. 1–41.

[2] D. N. Fittinghoff, P. R. Bolton, B. Chang, and K. C. Kulander, Phys. Rev. Lett. **69**, 2642 (1992).

[3] B. Walker *et al.*, Phys. Rev. A **48**, R894 (1993).

[4] V. V. Suran and I. P. Zapesochnyĭ, Pis'ma Zh. Tekh. Fiz. **1**, 973 (1975) [Sov. Tech. Phys. Lett. **1**, 420 (1975)].

[5] A. L'Huillier, L. A. Lompré, G. Mainfray, and C. Manus, Phys. Rev. Lett. **48**, 1814 (1982).

[6] D. Feldmann, H. J. Krautwald, and K. H. Welge, J. Phys. B **15**, L529 (1982).

[7] T. S. Luk *et al.*, Phys. Rev. Lett. **51**, 110 (1983).

[8] P. Agostini and G. Petite, J. Phys. B **18**, L281 (1985).

[9] L. F. DiMauro, Dalwoo Kim, M. W. Courtney, and M. Anselment, Phys. Rev. A **38**, 2388 (1988).

[10] Y. Zhu *et al.*, J. Phys. B **22**, 585 (1989).

[11] Y. L. Shao, V. Zafiropulos, A. P. Georgiadis, and C. Fotakis, Z. Phys. D **21**, 299 (1991).

[12] H. K. Haugen and H. Stapelfeldt, Phys. Rev. A **45**, 1847 (1992).

[13] I. S. Aleksakhin, N. B. Delone, I. P. Zapesochnyı, and V. V. Suran, Zh. Eksp. Teor. Fiz. **76**, 887 (1979) [Sov. Phys. JETP **49**, 447 (1979)].

[14] N. B. Delone, V. V. Suran, and B. A. Zon, in *Multiphoton Ionization of Atoms*, edited by S. L. Chin and P. Lambropoulos (Academic Press, Toronto, 1984), pp. 223–264.

[15] For the moment we disregard here the possible influence of ac Stark shifts of the levels involved, which can also lead to broadening and shifting of the electron energies observed.

[16] P. Lambropoulos, Phys. Rev. Lett. **55**, 2141 (1985).

[17] P. B. Corkum, Phys. Rev. Lett. **71**, 1994 (1993).

[18] D. A. Tate, D. G. Papaioannou, and T. F. Gallagher, J. Phys. B **24**, 1953 (1991).

[19] R. E. Bonanno, C. W. Clark, and T. B. Lucatorto, Phys. Rev. A **34**, 2082 (1986).

[20] P. Agostini and G. Petite, J. Phys. B **17**, L811 (1984).

[21] P. Camus *et al.*, J. Phys. B **22**, 445 (1989).

[22] I. I. Bondar' and V. V. Suran, Zh. Eksp. Teor. Fiz. **103**, 774 (1993) [Sov. Phys. JETP **76**, 381 (1993)].

[23] D. G. Papaioannou, D. A. Tate, and T. F. Gallagher, J. Phys. B **25**, 2517 (1992).

[24] D. Feldmann and K. H. Welge, J. Phys. B **15**, 1651 (1982).

[25] P. Agostini and G. Petite, Phys. Rev. A **32**, 3800 (1985).

[26] G. Petite and P. Agostini, J. Phys. (Paris) **47**, 795 (1986).

[27] Dalwoo Kim, S. Fournier, M. Saeed, and L. F. DiMauro, Phys. Rev. A **41**, 4966 (1990).

[28] X. Tang *et al.*, Phys. Rev. A **41**, 5265 (1990).

[29] J. O. Gaardsted *et al.*, J. Phys. B **24**, 4363 (1991).

[30] It seems likely that a recent claim of the observation of direct double ionization in barium with 40-ns 1-μm laser pulses [22] can also be explained in terms of competition of various paths for sequential double ionization.

[31] Meiying Hou, P. Breger, G. Petite, and P. Agostini, J. Phys. B **23**, L583 (1990).

[32] R. Trainham *et al.*, in *Coherence Phenomena in Atoms and Molecules in Laser Fields*, edited by A. D. Bandrauk and S. C. Wallace (Plenum Press, New York, 1992), pp. 1–10.

[33] W. C. Martin and R. Zalubas, J. Phys. Chem. Ref. Data **9**, 1 (1980).

[34] M. D. Lindsay *et al.*, Phys. Rev. A **45**, 231 (1992).

[35] Y. L. Shao, C. Fotakis, and D. Charalambidis, Phys. Rev. A **48**, 3636 (1993).

[36] P. Kruit and F. H. Read, J. Phys. E **16**, 313 (1983).

[37] L. D. Noordam *et al.*, Opt. Commun. **85**, 331 (1991).

[38] All electron energies in the equations have been calculated for $\hbar\omega = 2.1$ eV ($\lambda = 590.4$ nm), and without taking into account possible ac Stark shifts of the levels involved.

[39] I. I. Bondar and V. V. Suran, Opt. Spektrosk. **68**, 265 (1990) [Opt. Spectrosc. (USSR) **68**, 154 (1990)].

[40] D. G. Papaioannou and T. F. Gallagher, Phys. Rev. Lett. **69**, 3161 (1992).

[41] S. Kotochigova (private communication).

[42] The possibility of some Na^+ or Na^{2+} signal in the ion yield can be neglected, since the electron spectra taken at this intensity show no evidence for electrons resulting from ionization of sodium. In addition, as shown in the previous section, at lower intensities ($I = 2 \times 10^{12}$ W/cm^2) the ionization of sodium can already be neglected.

[43] T. N. Chang and X. Tang, Phys. Rev. A **46**, R2209 (1992).

[44] R. R. Freeman *et al.*, Phys. Rev. Lett. **59**, 1092 (1987).

[45] H. Rottke *et al.*, Phys. Rev. Lett. **64**, 404 (1990).

[46] R. B. Vrijen, J. H. Hoogenraad, H. G. Muller, and L. D. Noordam, Phys. Rev. Lett. **70**, 3016 (1993).

[47] A. A. Radzig and B. M. Smirnov, *Reference Data on*

Atoms, Molecules and Ions (Springer, Berlin, 1985).
[48] Liwen Pan, L. Armstrong, Jr., and J. H. Eberly, J. Opt. Soc. Am. B **3**, 1319 (1986).
[49] B. W. Shore, *The Theory of Coherent Atomic Excitation* (Wiley, New York, 1990).
[50] W. L. Wiese, M. W. Smith, and B. M. Miles, *Atomic Transition Probabilities* (U.S. GPO, Washington D.C., 1969).
[51] R. D. Cowan, *The Theory of Atomic Structure and Spectra* (University of California, Berkeley, 1981).
[52] E. U. Condon and G. H. Shortley, *The Theory of Atomic Spectra* (University Press, Cambridge, 1935).
[53] R. R. Freeman and P. H. Bucksbaum, J. Phys. B **24**, 325 (1991).
[54] H. B. Bebb, Phys. Rev. **149**, 25 (1966).

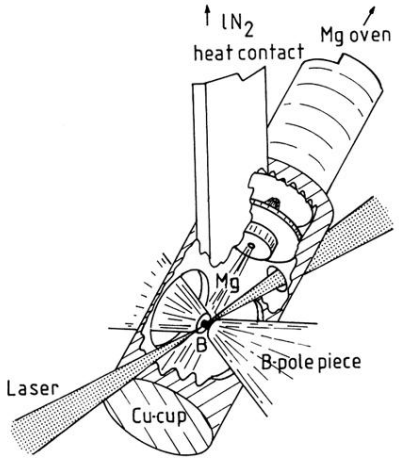

FIG. 2. The interaction region in the magnetic-bottle spectrometer. The laser beam crosses the magnesium atomic beam, and the resulting ions or electrons are detected. For electrons, the magnetic field serves to obtain a collection solid angle of 2π sr. The copper cup surrounding the interaction region is liquid nitrogen cooled, and captures the atomic beam.